Characterizing Multitemporal Alpine Snowmelt Patterns for Ecological Inferences

Abstract

Snowmelt patterns and the persistence of snowpatches into the growing season can profoundly affect the distribution of alpine vegetation. This study applies Markovian transition probability matrices to the problem of characterizing classified multitemporal satellite snow-cover data. Transition probability matrices are used to form hypotheses regarding the effects of snow persistence and ablation patterns on the alpine treeline using an integrated geographic information system. Four cloud-free Landsat MSS (Multispectral Scanner) scenes of a portion of Glacier National Park, Montana were processed to characterize periods of the 1987 snowmelt season. Stratification of the rugged landscape by elevation and slope aspect, achieved through the processing of 1:24,000 base-scale Digital Elevation Models (DEMs) and integrated with the satellite characterizations of snow conditions, demonstrated the dynamics of snow-cover conditions as a consequence of topographic position and antecedent snow conditions. Analysis of transition matrices by topographic position and watersheds highlighted areas of significantly late snowmelt, which holds implications for ecological investigations of alpine treeline by considering snow both as a stressor and protector of vegetation, depending upon its spatial pattern and temporal persistence.

Introduction

The general concept of seasonal snowmelt in alpine environments includes a gradual retreat of the snowline up the slopes of mountains as a consequence of seasonality, terrain orientation, and antecedent snow conditions. Regional and local biophysical factors operative on the landscape combine to modulate snowmelt patterns on a spatial and temporal basis, thereby yielding a dynamic landscape whose snow conditions can range from snow-covered, to snowpatch mosaic, to snow-free. The state of the snow landscape is spatially and temporally autocorrelated to prior snow-cover locations and phases of snowmelt morphology.

The spatial and temporal persistence of snow cover is an important factor affecting the composition and spatial patterns of alpine vegetation visible on the landscape. Depending upon the timing and spatial pattern of snow ablation, snow may function as a beneficial moisture reservoir, offer protection from climatic stresses, particularly wind dessication and ice abrasion, and serve as a cushion against disturbing forces such as snow avalanches (Billings, 1969; Canaday and Fonda, 1974; Butler and Malanson, 1985). Late-lying snow patches, however, can shorten the snow-free period available for vegetation establishment and growth by reducing flowering time, seeding rates, and seedling establishment (Billings and Bliss, 1959; Kudo, 1991; Kullmann, 1991). Lethal burial of saplings by thick snowpack may also depress the alpine treeline (Daly, 1984; Minnich, 1984). Further, the pattern and timing of snowmelt is important in determining soil and vegetation moisture levels which affect the alpine treeline by locally modulating possible drought conditions and fire fuels intensities and fire propensities (Kessell, 1979; Butler *et al.*, 1991).

The responses of alpine treeline components (closed-canopy forest, open-canopy forest, krummholz, meadow, and tundra) to local topoclimatic processes and disturbance regimes within Glacier National Park were modeled by Brown (1992) through four generalized linear models using logistic regression. Topoclimatic variables and disturbance factors formed the root independent variables, transformed through factor analysis, to model the location of the components of the alpine treeline ecotone. Spatial autocorrelation in the regression residuals indicated the presence of a pattern in the unexplained variance, thereby suggesting that other variables and processes were affecting the observed pattern of the alpine treeline not accounted for in the regression models.Brown (1992) suggested that possible regional and local basin controls on the alpine treeline were needed to improve model specification. Because local disturbance factors were statistically significant in the regression models, an expanded examination of snow accumulation and ablation patterns was initiated to improve the regional wind/snow accumulation parameter used in the regression models. A satellite-based multitemporal analysis of snow-cover conditions was implemented by deriving change probabilities of snow-cover conditions over time through change detection using transition probability matrices.

The basic intent of this research was to develop an approach for describing the temporal characteristics of snow accumulation and ablation patterns throughout a portion of Glacier National Park, Montana for formulating hypotheses regarding the variability in the observed position and character of the alpine treeline. The alpine treeline ecotone is a zone of transition that varies in three dimensions ranging from the closed-canopy forest to alpine tundra (Arno and Hammerly, 1984). This research sought to explore biophysical implications of snow patterns extending over time and space by generating Markov transition matrices for a snow-cover time-series for assessing changes in the state of seasonal snow conditions. The research employed Landsat mul-

Photogrammetric Engineering & Remote Sensing,
Vol. 59, No. 10, October 1993, pp. 1521–1529.

0099-1112/93/5910–1521$03.00/0

Thomas R. Allen
Stephen J. Walsh
Department of Geography, University of North Carolina,
Chapel Hill, NC 27599-3220.

tispectral scanner (MSS) satellite data to derive multitemporal landscape perspectives, a GIS to organize and integrate classified satellite data with digital terrain information derived from digital elevation models (DEMs), and Markovian transition probability analysis to quantify the transitions between snow conditions from successive satellite scenes. Elevation, slope aspect, and hydrologic basins were used to stratify the study area into biophysically significant aggregation units to examine spatial and temporal variations in snow-cover conditions that may influence the spatial and compositional variability of the alpine treeline ecotone.

Study Area

The study area is located in east-central Glacier National Park, Montana (Figure 1). This area consists of steep topography associated with Pleistocene and Holocene valley glacier advances. The climate in the Park is dominated by cold, snowy winters and brief, mild summers (Finklin, 1986). Elevations within the study area range from 1,400 m to more than 2,700 m. The bulk of the study area is located east of the Continental Divide where the climate is much harsher, with more severe low temperatures, stronger winds, and drier conditions as compared to sites west of the Divide (Finklin, 1986). In some areas the drier climate east of the Divide precluded glaciation during the late Pleistocene, leaving broad, gently sloping uplands in some locations above the present alpine treeline (Butler and Malanson, 1989). Strong winds redistribute snow within the study area, creating accumulation zones in cirques and hollows which protect snowfields and glaciers from direct solar radiation (Butler, 1989).

The alpine treeline within the study area is dominated by subalpine fir (*Abies lasiocarpa*), whitebark pine (*Pinus albicaulis*), and limber pine (*Pinus flexilis*). On the eastern side of the Divide, two treelines are evident: a drought-related treeline at low elevations and a temperature-related treeline at high elevations (Walsh *et al.*, 1989). The pattern of the alpine treeline is modulated in three dimensions owing to the pattern and type of disturbance and the spatial and biophysical factors affecting its site and situation. Snow-avalanche paths are striking disturbance features in the alpine and subalpine ecotones (Butler and Walsh, 1990). They combine with debris flows and fire disturbances to produce a landscape of substantial vegetative and geomorphic variability. Arno and Hammerly (1984) describe the alpine environment in the Park as a combination of extreme topographic and climatic stresses.

Background

One approach seldom used in biophysical remote sensing and GIS studies is to model temporal and spatial changes on the landscape as Markov processes, processes where changes between states or phases of land-cover conditions over time are linked to previous conditions through transition probabilities. In the area of landscape change simulation, Markov methods have been used in distributional and spatial landscape models (Baker, 1989). Markov methods have also been applied in ecological succession (Usher, 1981; Gibson *et al.*, 1983; Hobbs, 1983; Shugart *et al.*, 1988), in stratigraphic sequence simulation in sedimentology (Harbaugh and Bonham-Carter, 1981), and in remote sensing to measure forest changes after disturbance (Hall *et al.*, 1987). Markov models may incorporate spatial terms to account for spatial dependencies and have been used to simulate historical land-cover changes (Turner, 1988) and wetland vegetation succession (Sklar *et al.*, 1985).

Markov models describe the direction and rapidity of changes in systems. Represented in matrix form, transition matrices include rows of *from* states and columns of *to* states. A Markov transition matrix assumes a fixed number of

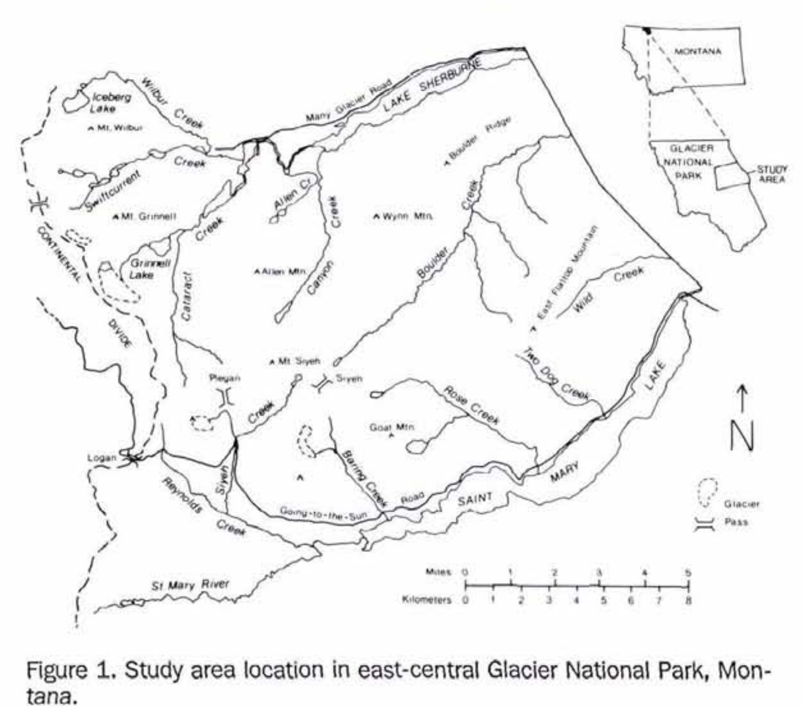

Figure 1. Study area location in east-central Glacier National Park, Montana.

states so that transitions between states can be described by a single matrix (Jeffers, 1985). In this research transition, probabilities are calculated from a tally matrix of pixels changing between three snow cover states based on classified Landsat MSS digital data: full snow cover, discontinuous snow cover, and snow-free. Given a tally matrix containing rows of *from* states and columns of *to* states, the calculation of transition probabilities for Markov analyses is given by

$$P_{ij} = \frac{a_{ij}}{\sum_{j=1}^{n} a_{ij}} \quad (1)$$

where P_{ij} is the probability of cell $i\,j$ of the transition matrix (Equation 2). The number of pixels changing from state i to j (a) is divided by the total of all changes from state i (a marginal total from the tally matrix). The general transition probability matrix derived from Equation 1 may be given by matrix **P** below: i.e.,

$$\mathbf{P} = \begin{bmatrix} P_{11} & P_{12} & P_{13} \\ P_{21} & P_{22} & P_{23} \\ P_{31} & P_{32} & P_{33} \end{bmatrix} \quad (2)$$

Note that the diagonal of the transition matrix (Equation 2) contains those elements which do not change and are referred to as retention probabilities. Assuming stationarity of the transition probabilities through time, a matrix can be powered to predict the state of the system n-time steps into the future. Order refers to the number of temporal steps contained in a Markov chain (Jeffers, 1985). All transition probabilities calculated in this research are first-order chains because transitions are between a single pair of successive satellite images that have been classified into three categories of snow: full snow cover, discontinuous or partial snow cover, and snow-free.

Because the transition probabilities based solely on temporal changes do not include spatial information besides total areas of change, spatial dependence within the system in question needs to be considered (Barringer and Robinson, 1981). Transition probabilities are not calculated on a per-pixel basis but on user-defined spatial aggregation units. In the most general derivation of a transition matrix, elements reflect all changes in the study area. Snow-cover patterns observed in Glacier National Park through the sampled data sets show a high degree of spatial order as indicated through the calculation of Moran's Index of spatial autocorrelation (first-order Rook's case autocorrelation for Moran's $I > 0.8$ for the classified snow-cover time series). The level of autocorrelation seen in the data largely results from the spatial structure of major glacial valleys as shown through semivariance analysis of DEMs (Bian and Walsh, 1993).It was found that, as snowmelt progressed, the index of spatial autocorrelation decreased, indicating the development of an increasingly discontinuous snow-cover pattern. Spatial dependence between successive scenes would be extremely important if Markov methods were to be used in an explicit spatial simulation of snowmelt.The use of Markov transition probability matrices for describing regional transition probabilities as used in this study, however, does not require such considerations. Rather than using matrices to predict future snow-cover patterns (inherently difficult given the nonstationarity of snowmelt processes), this research uses transition probability matrices, stratified by biophysically significant zones, to generate hypotheses regarding the effects of snowmelt pattern and timing on observed and expected patterns of the alpine treeline ecotone.

Methods

Background research on the climatology and snow-cover patterns for the study area were undertaken to assure that the satellite data for 1987 would be representative of general snowmelt patterns. Four Landsat Multispectral Scanner (MSS) digital data sets acquired for 4 April, 20 April, 6 May, and 7 June 1987, were used to assess snow-cover conditions throughout the study area. These dates were selected based upon cloud-free conditions over the study area for a near-normal snowfall year. Snow water equivalent (SWE) data for three snow courses located in the Park (Boulder Creek, Flattop Mountain, and Many Glacier) were plotted to compare 1961-1986 historical averages with data at the same three snow courses for the 1987 study period (USDA, SCS 1987) (Figure 2). The end points of the data indicate dates by which courses melted-out. Comparisons of the data indicate that 1987 ablated slightly earlier in the snowmelt season and that antecedent SWE conditions were slightly below the historical averages for all three courses. Boulder Creek (Figure 2a) and Flattop Mountain (Figure 2b) snow courses melted-

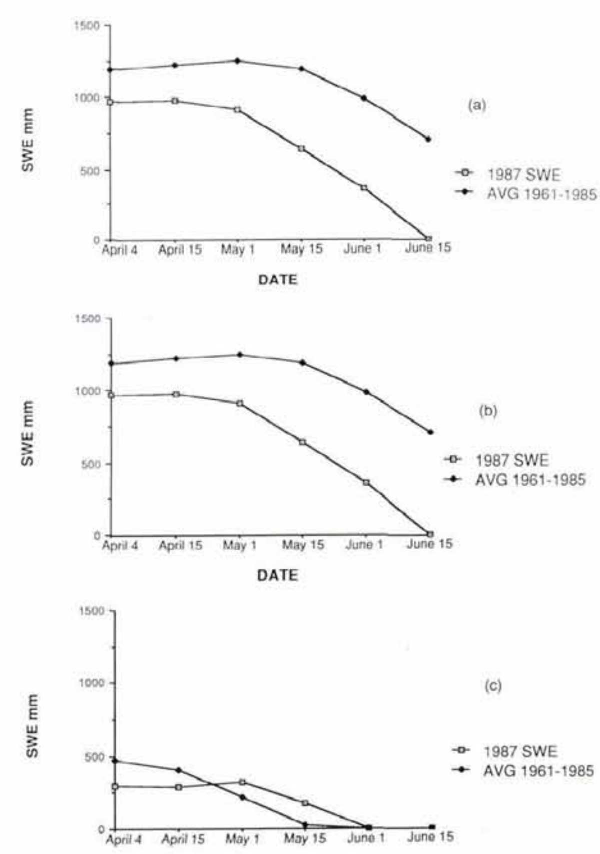

Figure 2. Comparison of snow-water equivalent (SWE) values (mm) of 1987 to the mean values from 1961-1985 for three snowcourses in Glacier National Park: (a) Boulder Creek, (b) Flattop Mountain, and (c) Many Glacier.

out at a near normal date. Many Glacier (Figure 2c) snow course also experienced a near normal melt-out although the majority of ablation was later in the measurement period. Variations between the snow courses indicate the relative accumulation and ablation differences due to topographic orientation and exposure. Figure 3 compares monthly snowfall averages for the historical record (1961-1985) and 1987 water year. The snowfall data corroborate the snow course assessment and further illustrate the heterogeneity of snowfall in this mountainous area. Overall, the data indicate that the 1987 snowmelt and ablation period was relatively normal despite an initially low snowfall in early and mid-winter (USDA SCS, 1987).

Following the atmospheric and radiometric corrections of each MSS image, the 7 June image was georeferenced to the UTM coordinate system (absolute georeference) using USGS 1:24,000-scale quadrangle maps and the ERDAS image processing software (ERDAS, 1993). An RMSE of approximately 0.5 pixel was achieved through the georeference procedures. Each of the other images was successively coregistered (relative georeference) to the June scene. The MSS data were resampled to a 50- by 50-m pixel for subsequent analysis and integration with other GIS data sets. The corrected MSS data sets were enhanced through channel ratios and principal components analysis (Walsh *et al.*, 1990) for possible integration with the MSS raw spectral channels for mapping snow conditions throughout the study area for each time period. The Landsat MSS ratio of channels 1 and 4 has been shown to effectively represent changes in snow-cover conditions (Thomas *et al.*, 1978). Comparisons were made between the unenhanced and enhanced spectral channels of the MSS data and known glaciers and semi-permanent snowfields occurring in the study area that were previously delineated through the use of USGS 1:24,000 scale topographic maps, 1:34,800-scale panchromatic (1966) and 1:58,000-scale color infrared (1987) aerial photography, terrestrial photography, and *in situ* field measurements represented within a GIS environment. The unenhanced spectral channels of Landsat MSS, however, were deemed sufficient for snow-cover mapping, given the rather general nature of the mapping requirements and the satisfactory differentiation of snow classes suggested by the initial inspection of enhanced and unenhanced spectral data for each time period.

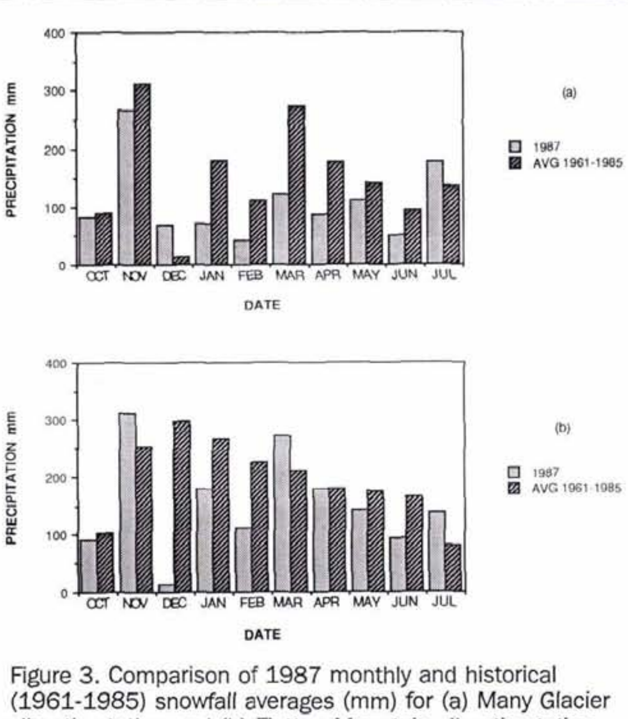

Figure 3. Comparison of 1987 monthly and historical (1961-1985) snowfall averages (mm) for (a) Many Glacier climatic station and (b) Flattop Mountain climatic station.

An unsupervised approach within ERDAS was used to independently classify each of the four Landsat MSS digital data sets. The ISODATA clustering technique was used to cluster the MSS spectral responses for snow-cover class designation and subsequent mapping. The ISODATA algorithm employs user-specific parameters (desired number of clusters, minimum number of pixels per cluster, and cluster iteration counter) to generate statistical clusters from the input spectral channels (Campbell, 1987; ERDAS, 1991; Walsh, 1993).The statistical clusters generated through the unsupervised approach for each data set were combined into snow-cover categories through the use of output statistics, image processing techniques, and field information and aerial photography.

Four landscape categories were used to represent the snow cover conditions for the 4 April and 20 April images, whereas six landscape categories were initially derived from the spectral clusters for the 6 May and 7 June images. The generation of additional landscape categories for the May and June images reflected the increasing spectral heterogeneity of the landscape as a consequence of a transition from full snow cover, to partial snow cover, to snow-free conditions, and the re-emergence of vegetation, particularly at the tree canopy level, in the pixel spectral responses. The defined spectral clusters for all the satellite data sets were merged to the same land-cover conditions and labeled to represent three identical landscape categories: full snow cover, discontinuous or partial snow cover, and snow-free conditions.

Each classified satellite image was transformed into an ERDAS GIS file (Figure 4). Using the GIS files for each date, an ERDAS GISMO program (GIS MOdeling: ERDAS, 1993) was written to retrieve and recode the temporal changes in the state of snow cover for each pixel and to create three nine-class change files for each pair of successive image dates. Using the three-class snow cover classification, the GISMO program recorded the frequencies of snow-cover changes in a 3- by 3-pixel (or tally) matrix from image differences between successive image dates (Plate 1). The derived values from the tally matrix were used to determine the transition probability matrix for each successive pair of image dates using Equation 1.

Transition Matrices

Accurate derivation of transition probability matrices is crucial to landscape change simulation using discrete time and discrete state models which define Markov Chains (Baker, 1989). As presented in Table 1, matrix [C1] is the transition probability matrix for snow-cover changes between 4 April and 20 April; matrix [C2] denotes transition probabilities between 20 April and 6 May; and matrix [C3] shows the transition probabilities for changes between 6 May and 7 June.

The transition matrices were tested for the Markov property, with the null hypothesis that transition probabilities were the results of a strictly random process. First-order Markov chains base the probabilities on changes between two successive dates (Jeffers, 1985). The first-order transition matrices were strongly Markovian because a dependence existed between the previous and succeeding snow cover

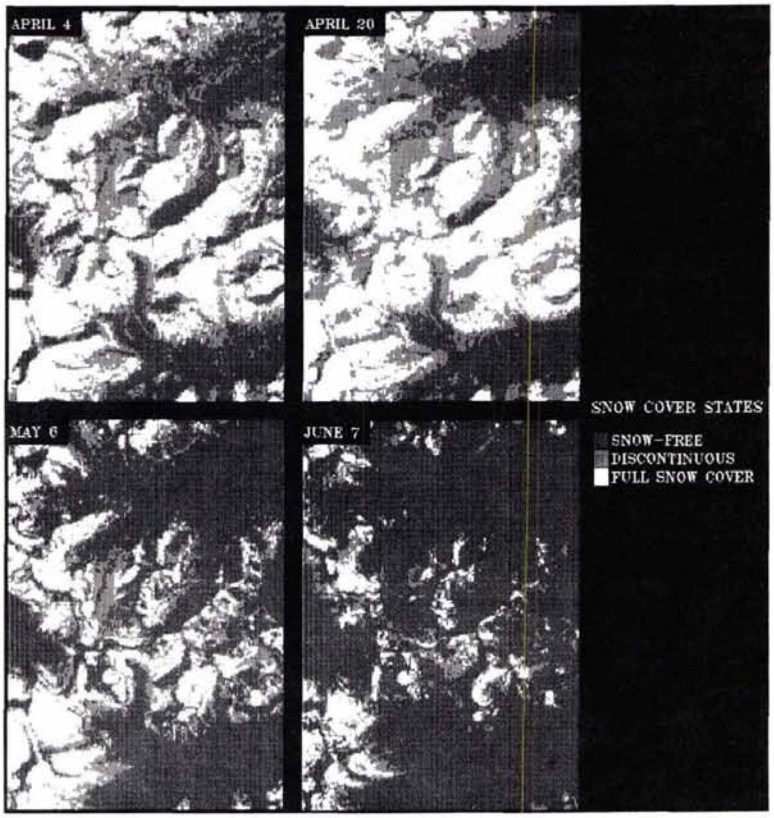

Figure 4. Classified snow-cover conditions for the four selected Landsat MSS scenes.

states. A test for higher order dependence was also found to be significant. An approach similar to Harbaugh and Bonham-Carter (1980) was used to test for double dependence in the snowmelt data in that transitions could be dependent on the initial conditions separated by two previous sequences in the time series. This test showed that snowmelt from 20 April to 6 May was not only dependent on conditions on 20 April, but also on conditions present on 4 April. The temporal relationship was tested through a chi-square approximation and was found statistically significant ($p=0.0001$); however, the similarity between the 4 April and 20 April images accounted for a high amount of that significance. Further, it became obvious that higher orders of dependence between successively earlier dates would generally indicate the increased likelihood of snow accumulation and not ablation. In addition, as a result of the influence of elevation on the transition probabilities of snow cover conditions, areas representing late snow accumulation would be the last areas that would meltout, as reflected in the selected satellite time series.

Transition probability matrices were used for characterizing retention probabilities, the probability that a pixel will remain in the same state over time, indicated by the diagonal of the transition matrix (Hall *et al.*, 1987). These transition values show the temporal dynamics of snowmelt. The diagonals of the original transition matrices (Table 1), show that full snow cover tended to remain in that state from 4 April through 20 April [C1] ($p=0.883$), whereas partially snow-covered pixels showed a much lower retention probability by the 20 April to 6 May sequence [C2] ($p=0.201$). Snow-free areas tended to increase the retention probability of that state by the second period (20 April to 6 May) ($p=0.997$) although the probability value decreased very slightly in the [C3] sequence ($p=0.986$), possibly in response to localized wind redistribution of snow. These retention probabilities agreed with the general retreat of the snowline and the normal reduction in the size of snowpatches as snow-free areas expanded. The transition probabilities for the discontinuous or partial snow-cover class were similar to the probabilities for the full snow-cover class rather than the snow-free class – a decreasing retention probability over time (p-value range from 0.623, to 0.201, to 0.162). The increase of discontinuous or partial snow cover relative to full snow cover through the season reflects the changing scale of terrain effects as snowmelt progresses. This corroborates the general model of snowline changing from zonal to azonal with increasing patchiness as snow ablation continues (Minnich, 1984).

The technique of assessing the transition matrices simultaneously while viewing the satellite images used to derive the matrices was a useful approach for understanding the rate and pattern of snowmelt within the study area. For instance, an interpretation of matrix [C1] (Table 1a) indicates that snowfall occurred in the study area between the periods 4 April and 20 April. That observation was corroborated through snowfall data collected at climatic recording stations and snow courses located within and surrounding the study area (Figures 2 and 3). The probability of changing from snow-free to partial snow cover ($p=0.325$) was much higher

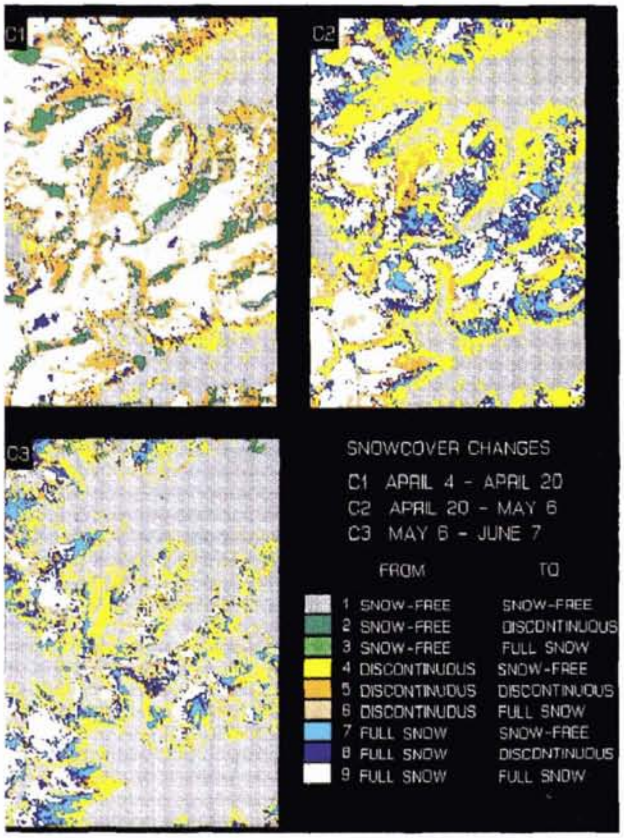

Plate 1. Snow-cover change images used to derive Markov transition probabilities.

Table 1. Snow-Cover Transition Probability Matrices for the Entire Study Area.

	(a) To (20 April): Full	Discontinuous	Snow-Free
From (4 April)			
Full	0.883	0.114	0.003
Discontinuous	0.233	0.623	0.144
Snow-Free	0.014	0.325	0.662
	(b) To (6 May): Full	Discontinuous	Snow-Free
From (20 April):			
Full	0.497	0.299	0.204
Discontinuous	0.048	0.201	0.744
Snow-Free	0.001	0.002	0.997
	(c) To (7 June): Full	Discontinuous	Snow-Free
From (6 May):			
Full	0.365	0.318	0.317
Discontinuous	0.018	0.162	0.821
Snow-Free	0.003	0.011	0.986

than would be expected if snow steadily melted without additional snowfall occurring during the two time periods.

Similarly, the transition from discontinuous to full snow cover was relatively high (p=0.233) for the period of 4 April through 20 April which further suggested that snowfall occurred between the two dates evaluated. The retention probability value for snow-covered areas (p=0.883) suggested that full snow cover remained stable over this time span. The Markov transition matrix showed that most of the change in the study area was towards the net accumulation of snow, both partially covered and fully covered areas.

In the [C2] transition matrix (Table 1b), representing snow-cover changes between 20 April and 6 May, the typical timing of snowmelt is presented. The dynamics of snow-cover change between these dates shows a transition from full snow cover, to partial snow cover, to snow-free states. Indeed, the probability of changing from full snow cover to discontinuous or partial snow cover and snow-free conditions increased from a combined probability of 0.117 for [C1] to 0.503 for [C2], reflecting the accelerated pace of ablation. Further, the probability of pixels classified as discontinuous or partial snow cover becoming snow-free was 0.744. By time step three (7 June, [C3], Table 1c), the probability vector showed a distinct snow ablation trend with a high transition of snow-covered areas towards discontinuous (p=0.318) and snow-free conditions (p=0.317).

To develop snow-cover transition relationships beyond the final satellite image acquired on 7 June, matrix [C3] could be powered successively higher to yield predicted distributions of snow-cover change; however, such powering of Markov matrices requires an assumption that the transition probabilities are stationary, indicating a constant rate of snow ablation through time. As illustrated by the three matrices ([C1], [C2], and [C3]), the probability values changed as a consequence of the biophysical processes affecting snow accumulation and ablation rates and magnitudes. As snowmelt ceases, the transition probabilities will stabilize until the cycle of snowfall begins anew.

Terrain Stratification

Generating probability matrices for landscape units (e.g., elevation zones, watersheds, plant communities, and ecotones) can be used to further explore spatial and temporal patterns of phenomena. In this research, the landscape was categorized into ecologically significant elevation zones that affected vegetation composition and ecological gradients within the study area to explore the relationship between snow patterns and the alpine treeline. The elevation values, represented on a series of 1:24,000 base-scale digital elevation models (DEMs), were resampled to a 50- by 50-m cell size and then recoded into elevation zones through use of the ERDAS GIS software. The five elevation zones range from 1600 to 2600 m with equal intervals: (1) 1600 to 1800 m; (2) 1801 to 2000m; (3) 2001 to 2200m; (4) 2201 to 2400m; and (5) greater than 2400m. Brown (1992) reported that elevation was a primary control of the alpine treeline within the Park and that such aggregations of elevation values significantly explained vegetation components of treeline transitions. Figure 5 shows the seasonal snow cover changes for the five elevation zones evaluated. This figure illustrates the overall ablation (which includes snowmelt as well as losses from evaporation and sublimation) within and between the elevation zones. The transition matrices for each zone indicate the expected trend of meltout temporally related to elevation — lower sites being more prone to earlier meltout than higher sites.

It should be noted that, because a transition matrix must be generated for each zone and for each time sequence, difficulties in interpretation arise from the increased number of

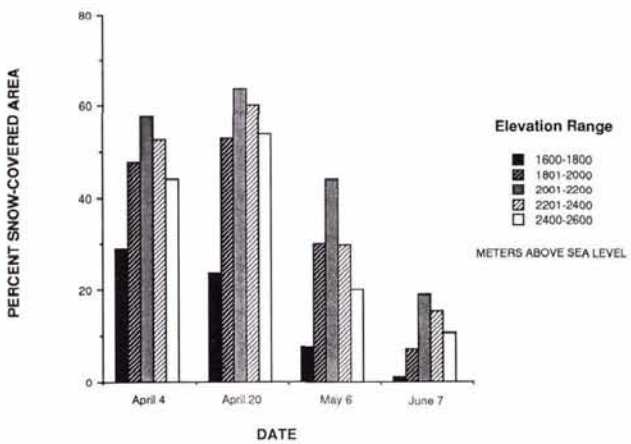

Figure 5. Seasonal snow-cover changes derived for selected elevation zones.

TABLE 2. PROBABILITY OF SNOW ABLATION BY ELEVATION ZONES.

Elevation Zone (m)	Time Period [C1] 4 April–20 April	[C2] 20 April–6 May	[C3] 6 May–7 June
1600-1800	0.155	0.509	0.239
1801-2000	0.054	0.493	0.476
2001-2200	0.042	0.427	0.437
2201-2400	0.038	0.578	0.332
>2400	0.021	0.667	0.281

matrices. Rather than attempt an interpretation of the entire set of matrices, only specific probability vectors and retention probabilities are analyzed here to show the potential of this approach. By summing the probabilities of decreasing snow cover (transition from snow to discontinuous or snow-free conditions, and transition from discontinuous to snow-free conditions) from the elevation zone matrices, the overall probability of ablation was derived (Table 2). The probabilities listed in Table 2 show marked variation. In the first period, 4 April to 20 April, the lowest elevation has the highest probability of ablation during this period, which was just prior to pronounced snowmelt. The snowfall event in this period possibly precluded accumulation at the lower elevations. Period [C2] shows a general trend of increasing ablation probability with elevation (from 0.5 to 0.67), possibly indicating the influence of wind (which increases with exposure and elevation) on redistribution, evaporation, and sublimation of snowpatches. Vegetation corresponding to this zone includes low and medium density forests and meadows. In the final sequence, the highest ablation probabilities occurred in the middle elevation zones from 1800 to 2200 m. This zone corresponds primarily to meadow and alpine tundra communities. Therefore, the elevation-stratified Markov analysis suggested that the timing of snowmelt is a possible variable for inclusion in future modeling of alpine vegetation communities. Such a time-dependent variable imparts to the analysis a perspective of snow beyond the presence or absence discerned from static single-scene analyses.

The landscape was also characterized by eight equal slope aspect categories, also derived from the series of 1:24,000 base-scale DEMs. Markov transition matrices generated for each aspect class indicated the differential accumulation and ablation of snow that occurs as a function of terrain orientation. Probabilities in Figure 6 were derived by combining the probabilities of changing from snow-free to discontinuous or full snow cover conditions and from discontinuous to full snow cover conditions to generate general probabilities of increases in snow cover. Figure 6 shows, for example, higher likelihoods of northwest- to northeast-facing slopes in receiving snow accumulation from 4 April to 20 April based on transition probabilities plotted on a star diagram.

As a final stratification technique, the study area was subdivided into watersheds for interbasin comparisons. Watersheds were defined on USGS 1:24,000-scale topographic maps and digitized in a raster GIS format. Three watersheds were selected having different orientations and proximities to the Continental Divide. The outlet of Baring Creek basin is oriented towards the southeast; Siyeh Creek basin towards the south; and Cataract Creek basin towards the north (Figure 1). Differences in snow accumulation, solar insolation, and wind exposures were expected to be observable in snowmelt regimes as quantified through Markov transition matrices as a consequence of basin orientations and observed summer field conditions. Brown (1992) reported that differences between the observed and expected position of the alpine treeline were greatest in these watersheds. He suggested that local disturbance factors were responsible for the higher model residuals.

Analysis of the percent snow-covered area by basin provides comparative information on the relative timing and intensity of snowmelt. The retention probabilities provide further information as to the relative changes of snow-cover states. For 4 April to 20 April, Baring basin has a strikingly high retention of snow-free areas and the lowest probability of new snow accumulation, suggesting that the basin's distance from the Continental Divide may place the basin in a "snow shadow" relative to the other two basins. In fact, Baring basin exhibits the earliest snowmelt by comparison to Siyeh and Cataract basins, and decreases in percent snow-covered area between 4 April and 20 April. Cataract basin, on the other hand, has the latest overall meltout of the three basins, as would be expected from its northerly orientation. Further, several snowpatches remain on the eastern flank of

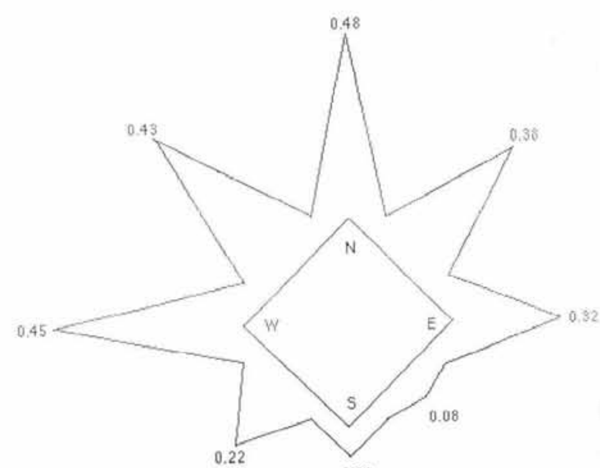

Figure 6. Probability of increasing snow cover by slope aspect zones.

this watershed by the 7 June image. In Siyeh basin, snowmelt is intermediate between the transitions in Baring and Cataract basins. In the 20 April to 6 May sequence, Baring basin has the highest meltout probabilities (0.85 discontinuous to snow-free conditions and 0.67 full snow to discontinuous snow cover conditions). Siyeh and Cataract basins have approximately equal probabilities of meltout for this time period. By the final sequence (6 May to 7 June), Cataract and Siyeh basins have much higher ablation probabilities, and Baring basin shows a deceleration of snowmelt (indicated by a high retention probability for full snow cover (0.44), likely a result of the large cirque form of the upper basin which includes Sexton Glacier). Interannual trends could be further quantified to compare the representativeness of 1987 patterns of snowmelt for characterizing snowmelt variability.

The spatial-temporal patterns for the three selected basins suggest that ecological effects of snow cover may be controlling the distribution of treeline components in these three basins. For example, the early lower elevation meltout in Baring basin exposes the treeline ecotone to dessicating winds in early spring, a possible explanation for the depressed treeline noted in that watershed. Further, the observed lag in snowmelt and persistence of large snowpatches into the summer (occurring after the 7 June satellite image) could significantly shorten the growing season in Cataract basin, possibly accounting for the depressed treeline ecotone in that basin (Brown, 1992). Finally, the intermediate snowmelt date and pattern in Siyeh basin may represent a condition where snow lingers sufficiently long to protect vegetation from wind dessication while melting early enough to allow spring-summer vegetative growth. This would partially explain the unexpected occurrence of the treeline in the high elevations of the Preston Park area of Siyeh Creek basin (Brown, 1992). While the interpretation of the transition probabilities applied to questions of alpine treeline patterns in three dimensions cannot be rigorously tested using the constrained Markovian approach, the use of Markov transition probabilities has been useful to characterize the timing of snowmelt as well as the spatial pattern and to suggest several hypotheses regarding the impact of snow accumulation and ablation patterns on alpine vegetation.

Conclusions

Landscape changes, evaluated through multitemporal satellite data, can be quantitatively assessed through the application of transition probability matrices. Transition probability matrices proved useful in quantifying snowmelt timing and the pattern of that change among snow cover classes. Markovian transition probability matrices were used to characterize the observed fluctuation and subsequent acceleration of spring snowmelt within the study area. The landscape was stratified into zones of elevation and slope aspect for change assessment and for evaluating the relative dynamism of change along environmental gradients. Distinct differences in the onset and pattern of snowmelt among the three watersheds suggest that snowmelt patterns may be affecting environmental gradients and forcing a response of the alpine treeline ecotone based on timing and pattern of snowmelt.

Hypotheses are being generated to aid in the interpretion of the transition matrices, particularly for differences in accumulation and ablation patterns derived for watersheds. Variables that could be generated to explore possible biophysical processes accounting for snow pattern and timing differences and, hence, variability of the alpine treeline ecotone include basin orientation and symmetry; intervening topography affecting shadow and microclimate; topographic situation of the basin relative to the Continental Divide; slope position (upslope, mid-slope, down-slope) and slope form (convex or concave) within basins and differences between basins; surface roughness and slope orientations within basins; proportion of vegetation types within basins and their spatial patterns; basin proximity to the range front; and the spatial linkage of disturbances such as snow-avalanche paths and debris flows with basin snow accumulation potential and snowmelt timing.

The integration of space and time dimensions has been relatively neglected in biophysical studies involving landscape processes and for explaining differences between observed and expected distributions. Biophysical studies are seldom conducted that use techniques that reflect an integration of *from* state and *to* state information for further hypothesis generation. In this particular study, information generated from the transition matrices has suggested the inclusion of variables operating at particular temporal and spatial scales that may be important factors in understanding alpine treeline spatial variability. Transition matrices, combined with remote sensing and GIS techniques, can yield an effective approach for landscape characterization that represents landscape change as a critical descriptor variable.

References

Arno, S. F., and R.P. Hammerly, 1984. *Timberline, Mountain and Arctic Forest Frontiers*, The Mountaineers, Seattle, Washington.

Baker, W.L., 1989. A review of models of landscape change, *Landscape Ecology*, 2(2):111-133.

Barringer, T.H., and V.B. Robinson, 1981. Stochastic models of cover class dynamics, *Proceedings, Fifth International Symposium on Remote Sensing of Environment*, pp. 125-144.

Bian, L., and S.J. Walsh, 1993. Scale dependencies of vegetation and topography in a mountainous environment of Montana, *Professional Geographer*, 45(1):1-11.

Billings, W. D., 1969. Vegetational pattern near alpine timberline as affected by fire-snowdrift interactions, *Vegetatio*, 19:192-207.

Billings, W.D., and L.C. Bliss, 1959. An alpine snowbank and its effects on vegetation, plant development, and productivity, *Ecology*, 40(3):388-397.

Birnie, R.V., 1986. Pixel-mixing effects and their significance to identifying snow condition from Landsat MSS Data, *International Journal of Remote Sensing*, 7(7):845-853.

Brown, D.G., 1992. *Topographical and Biophysical Modeling of Vegetation Patterns at Alpine Treeline*, Unpublished Ph.D. Dissertation, University of North Carolina at Chapel Hill.

Butler, D.R., 1989. Glacial hazards in Glacier National Park, Montana, *Physical Geography*, 10(1):53-71.

Butler, D. R., and G.P. Malanson, 1985. A history of high-magnitude snow avalanches, southern Glacier National Park, Montana, USA, *Mountain Research and Development*, 5(2):175-182.

———, 1989. Periglacial patterned ground, Waterton-Glacier International Peace Park, Canada and U.S.A., *Zeitschrift für Geomorphologie*, 33(1):43-57.

Butler, D. R., and S.J. Walsh, 1990. Lithologic, structural, and topographic influences on snow-avalanche path location, eastern Glacier National Park, Montana, *Annals of the Association of American Geographers*, 80(3):362-378.

Butler, D. R., S.J. Walsh, and G.P. Malanson, 1991. GIS applications to the indirect effects of forest fires in mountainous terrain, *Fire and the Environment: Ecological and Cultural Perspectives* (S.C. Nodvin and T.A. Waldrop, editors), Southeast Forest Experiment Station, Asheville, North Carolina, pp. 202-211.

Campbell, J. B., 1987. *Introduction to Remote Sensing*, The Guilford Press, New York, 551 p.

Canaday, B. B., and R.W. Fonda, 1974. The influence of subalpine snowbanks on vegetation pattern, production, and phenology, *Bulletin of the Torrey Botanical Club*, 101(6):340-350.

Daly, C., 1984. Snow distribution patterns in the alpine krummholz zone, *Physical Geography*, 8:157-175.

Finklin, A.I., 1986. *A Climatic Handbook for Glacier National Park-With Data for Waterton Lakes National Park*, Intermountain Research Station, USDA Forest Service, General Technical Report INT-204, 124 p.

Frank, T.D., 1988. Mapping dominant vegetation communities in the Colorado Front Range with Landsat Thematic Mapper and digital terrain data, *Photogrammetric Engineering & Remote Sensing*, 54(12):1727-1734.

Gibson, C.W.D., T.C. Guilford, C. Hambler, and P.H. Sterling, 1983. Transition matrix models and succession after release from grazing on Aldabra Atoll, *Vegetatio*, 52:151-159.

Hall, D.K., W.M. Kovalcik, and A.T.C. Chang, 1990. Satellite-derived reflectance of snow-covered surfaces in northern Minnesota, *Remote Sensing of Environment*, 33:87-96.

Hall, F.G., D.E. Strebel, S.J. Goetz, K.D. Woods, and D.B. Botkin, 1987. Landscape pattern and successional dynamics in the boreal forest, *Proceedings, IGARSS '87 Symposium*, Ann Arbor, Michigan, pp. 473-482.

Harbaugh, J.W., and G. Bonham-Carter, 1981. *Computer Simulation in Geology*, Wiley-Interscience, New York, 575 p.

Hobbs, R.J., 1983. Markov models in the study of post-fire succession in heathland communities, *Vegetatio*, 56:17-30.

Jeffers, J.N.R., 1988. *Practitioners Handbook on the Modelling of Dynamic Change in Ecosystems*, Scientific Committee on Problems of the Environment (SCOPE), 34, 181 p.

Kessell, S. R., 1979. *Gradient Modeling: Resource and Fire Management*, Springer-Verlag, New York.

Kudo, G., 1991. Effects of snow-free period on the phenology of alpine plants inhabiting snow patches, *Arctic and Alpine Research*, 23(4):436-443.

Kullmann, L., 1991. Ground frost restriction of subarctic Picea abies forest in northern Sweden: A dendroecological analysis, *Geografiska Annaler*, 73A(3-4):167-178.

Minnich, R.A., 1984. Snow drifting and timberline dynamics on Mount San Gorgonio, California, U.S.A., *Arctic and Alpine Research*, 16(4):395-412.

Shugart, H.H., P.J. Michaels, T.M. Smith, D.A. Weinstein, and E.B. Rastetter, 1988. Simulation models of forest succession, *Scales and Global Change* (T. Rosswall, R.G. Woodmansee, and P.G. Risser, editors), pp. 125-151.

Sklar, F.H., R. Costanza, and J.W. Day, Jr., 1985. Dynamic spatial simulation modeling of coastal wetland habitat succession, *Ecological Modeling*, 29:261-281.

Thomas, I.L., A.J. Lewis, and N.P. Ching, 1978. Snowfield assessment from Landsat, *Photogrammetric Engineering & Remote Sensing*, 44(4):493-502.

Turner, M.G., 1988. A spatial simulation model of land use changes in a piedmont county in Georgia, *Applied Mathematics and Computation*, 27:39-51.

Usher, M.B., 1981. Modeling ecological succession, with particular reference to Markovian models, *Vegetatio*, 46:11-18.

U.S.D.A. Soil Conservation Service, Snow Survey Unit, 1987. *Montana Annual Data Summary of Federal-State-Private Cooperative Snow Surveys*, 42 p.

Walsh, S. J., 1993. Spatial and biophysical analysis of alpine vegetation through Landsat TM and SPOT MX/PAN data, *Proceedings, American Congress on Surveying and Mapping and American Society for Photogrammetry and Remote Sensing Annual Convention*, New Orleans, Louisiana, 2:426-437

Walsh, S. J., L. Bian, D.G. Brown, D.R. Butler, and G.P. Malanson, 1989. Image enhancement of Landsat Thematic Mapper digital data for terrain evaluation, Glacier National Park, Montana, USA, *Geocarto International*, 3:55-58.

Walsh, S. J., J. W. Cooper, I. E. Von Essen, and K. R. Gallager, 1990. Image Enhancement of Landsat Thematic Mapper Data and GIS Data Integration for Evaluation of Resource Characteristics, *Photogrammetric Engineering & Remote Sensing*, 56(8):1135-1141.